

Swirl ratio effects on tornado vortices in relation to the Fujita scale

H. Hangan* and J-D. Kim

*Alan G. Davenport Wind Engineering Group, The Boundary Layer Wind Tunnel Laboratory,
The University of Western Ontario, Faculty of Engineering, London, Ontario, Canada*

(Received October 1, 2007, Accepted June 18, 2008)

Abstract. Three-dimensional engineering simulations of momentum-driven tornado-like vortices are conducted to investigate the flow dynamics dependency on swirl ratio and the possible relation with real tornado Fujita scales. Numerical results are benchmarked against the laboratory experimental results of Baker (1981) for a fixed swirl ratio: $S = 0.28$. The simulations are then extended for higher swirl ratios up to $S = 2$ and the variation of the velocity and pressure flow fields are observed. The flow evolves from the formation of a laminar vortex at low swirl ratio to turbulent vortex breakdown, followed by the vortex touch down at higher swirls. The high swirl ratios results are further matched with full scale data from the Spencer, South Dakota F4 tornado of May 30, 1998 (Sarkar, *et al.* 2005) and approximate velocity and length scales are determined.

Keywords: tornado-like vortices; swirl ratio; Fujita scale.

1. Introduction

Between 52% and 75% of the extreme annual winds in South-Central United States were registered on thunderdays (Twisdale and Vickery 1992), and 66% of all high intensity wind (HIW) events in North Eastern United States involving damaging effects on buildings and structures are associated with thunderstorms (based on unpublished recent reports). One of the main HIW events accompanying thunderstorms are tornados.

A tornado is a “highly convergent swirling wind affecting a relative narrow path”, (Fujita 1981). The tornado size measured by the path width has average values of approx. 550 meters for F5 tornadoes (Brooks 2004) but can reach extremes of up to 4,000 meters, see SPC website (<http://www.spc.noaa.gov>) for the Hallam, Nebraska F4 tornado of 22 May 2004. The complex flow structure of tornado vortices depends mainly on the swirl ratio, i.e., the ratio between the initial swirl and radial velocities in the flow.

Radar observed field measurements of real tornadoes were used to investigate details of tornado flow fields (Wurman and Gill 2000, Bluestein, *et al.* 2004). However, a full scale quantitative spatial and temporal data for tornado winds mostly for the near ground region (of interest for wind engineering applications) is still lacking. Only recently, detailed field data has been obtained for the

* Associate Professor and Research Director, Corresponding Author, E-mail: hmh@blwtl.uwo.ca

Spencer, South Dakota F4 tornado of May 30, 1998 (Sarkar, *et al.* 2005) and for the Mulhall F4 tornado of May 3, 1999 (Lee and Wurman 2005)

Given the difficulty in gathering full-scale data, laboratory simulations have been directed so far towards generic experiments of tornado-like vortices in Tornado Vortex Chambers (TVC) (Wan and Chang 1972, Ward 1972, Davies-Jones 1973, Church, *et al.* 1977, Baker and Church 1979, Church, *et al.* 1979, Rotunno 1979, Lund and Snow 1993, Wang, *et al.* 2001, Sarkar, *et al.* 2005).

The main dimensionless parameters governing these laboratory tornado-like vortices are the aspect ratio $AR = r_0/h_0$, where r_0 is a characteristic radius usually corresponding to maximum tangential velocity at certain height and h_0 is a height that usually corresponds to uniform axial velocity, the swirl ratio, $S = V_t/2V_r$ (where V_t is the tangential inflow velocity at r_0 and V_r the axial velocity at r_0), the Reynolds number $Re = (V_r r_0)/\nu$ and the Froude number $Fr = ((\Delta p/2g\Delta ph)^{1/2})$. Laboratory (e.g. Ward 1972, Church, *et al.* 1979, Snow 1982) and numerical studies (e.g. Lewellen 1963, Davies-Jones 1973) have shown that the swirl ratio is the dominant governing parameter. Fig. 1, reproduced from Lugt (1989), portrays some of the flow patterns for increasing swirl ratio.

Indeed, with increasing swirl the tornado vortex evolves from a jet-like flow, to a one-cell vortex, Fig. 1(a), followed by the formation of a stagnation point and vortex break down aloft, Fig. 1(b), touch down and two-cell vortex formation, Fig. 1(c). Finally at high swirl ratio multiple vortices develop from an instability of the cylindrical shear layers (Davies-Jones 1973, Church, *et al.* 1979, Fiedler and Rotunno 1986).

While the TVC experiments provide some inside in the tornado-like-vortex phenomena there are few quantitative studies that provide a complete characterization of the associated velocity and pressure fields. Moreover, the laboratory data is affected by the presence of the boundaries of the experimental apparatus, (Smith 1987) and it is usually limited to small scales and rather small variations of the swirl ratio. While Lewellen, *et al.* (2000) argued that for real tornados the correlation between swirl and flow patterns is more problematic Lee and Wurman (2005), for instance, observed that for the F4 Mulhall tornado the computed swirl ratios between 2 and 6 were consistent with the observed multiple vortex radar signatures.

Extensive numerical simulations of tornadoes have also been performed, e.g. Lewellen, *et al.* (1997, 2000), Xia, *et al.* (2003), Lewellen and Lewellen (2007) mostly as meteorological type simulations. Most of these models take into account large scale atmospheric motions that include thermodynamic and moisture fields reproducing various aspects of the tornado-genesis or detailing important flow features. Engineering numerical models of tornado-like vortices whilst sacrificing some of these atmospheric features (and therefore not questioning the tornado-genesis) have the advantage of being similar with laboratory fluid mechanics experiments and therefore allow for benchmarking. At the same time these are scaled models and therefore allow for grid refinement in the near-surface region which is of interest to wind engineering applications. Such models of tornados and their effects on low-rise buildings have been attempted (Selvam and Millet 2003, 2005) but without investigating the effect of swirl ratio on the flow field or the possible relation between swirl ratio, a fluid mechanics parameter, and the extensively used Fujita scale, a forensic parameter.

While tornados are complex in nature, and there is no one-to-one relation between swirl in laboratory or numerical simulations and the Fujita scale our focus herein is on how one can relate engineering laboratory and numerical models (mainly governed by swirl ratio) to field tornados characterized by the forensic Fujita scale. By comparing the numerical results to recent full-scale tornado data we attempt establishing such a relation. The focus is on practical, engineering scaling

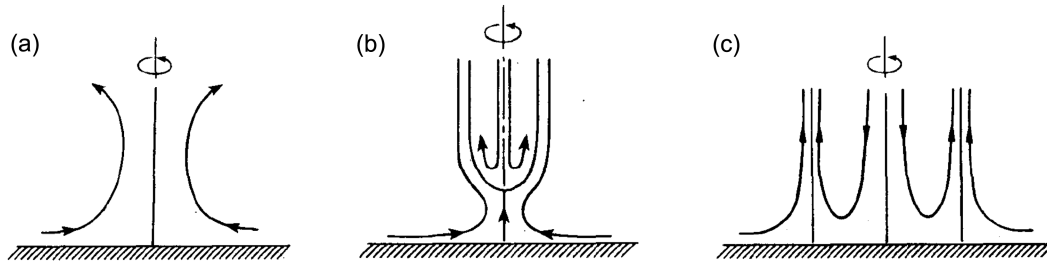


Fig. 1 Various flow patterns in a tornado with increasing swirl (S) ratio, reproduced from Lugt (1989)

aspects rather than the in-depth but qualitative description of tornado-like vortex structure.

Stationary tornadoes of various swirl ratios are simulated solving two-dimensional (axisymmetric) and three-dimensional Reynolds Averaged Navier-Stokes (RANS) equations. These simulations are benchmarked against the TVC experimental results of Baker (1981) for a fixed swirl ratio $S=0.28$ followed by an extension of the numerical results up to $S=2$. The flow dependency on swirl ratio is investigated in terms of velocity and pressure fields. The high swirl ratio results are then matched with full scale data from the Spencer, South Dakota F4 tornado of May 30, 1998 and an attempt is made to establish a first possible relation between swirl ratio and Fujita scale.

2. Numerical set-up and benchmarking

2.1. Numerical set-up

The study uses the commercially available numerical platform FLUENT 6.2 to investigate the flow characteristics of laboratory scale tornado vortices. Considering that the flow is symmetric in the azimuthal direction, an unsteady two-dimensional (2D) axisymmetric turbulent swirl flow was simulated first. While this is a good preliminary approach, it is known that tornado vortices develop a spiral instability that leads to vortex funnel breakdown (Lim and Cui 2003, Serre and Boutoux 2002). Therefore three-dimensional (3D) simulations were conducted in a second stage. Fig. 2 shows the schematic diagrams of the computational domain and boundary conditions. X-axis corresponds to the radial direction and Z-axis corresponds to the axial or vertical direction, respectively. The size of the two-dimensional computational domain was $(r_0, h_0) = (0.4 \text{ m}, 0.4 \text{ m})$, similar to that of Wilson and Rotunno (1986). Based on the preliminary 2D study of the influence of boundaries the size of the three-dimensional domain was increased to $(r_0, h_0) = (0.6 \text{ m}, 0.6 \text{ m})$.

Unsteady Reynolds Averaged Navier-Stokes (RANS) equations are solved on structured grids for various swirl ratios between $S=0.1$ and $S=2.0$. Following an initial grid convergence analysis, structured grids comprising 54659 cells for 2D simulation and 152538 cells for 3D simulations were used for swirl ratio $S=0.28$ for which the experiments of Baker (1981) were available for benchmarking. For the 3D simulations the size of the control volumes varies between 7×10^{-7} to $2 \times 10^{-10} \text{ m}^3$. A Reynolds Stress Model (RSM) is used with model constants as follows: $C_\mu = 0.09$; $C_{1\varepsilon} = 1.44$; $C_{2\varepsilon} = 1.92$; $C_{1-ps} = 1.8$; $C_{2-ps} = 0.6$; $C_{1'-ps} = 0.5$, $C_{2'-ps} = 0.3$, Turbulent kinetic energy (TKE) Prandtl number = 1; Turbulent dissipation rate (TDR) Prandtl Number = 1.3. While for swirling flows, the redistribution of turbulence by fluctuating pressure is indeed different compared to non-swirling flows a vast range of constants have been suggested by several researchers. Most

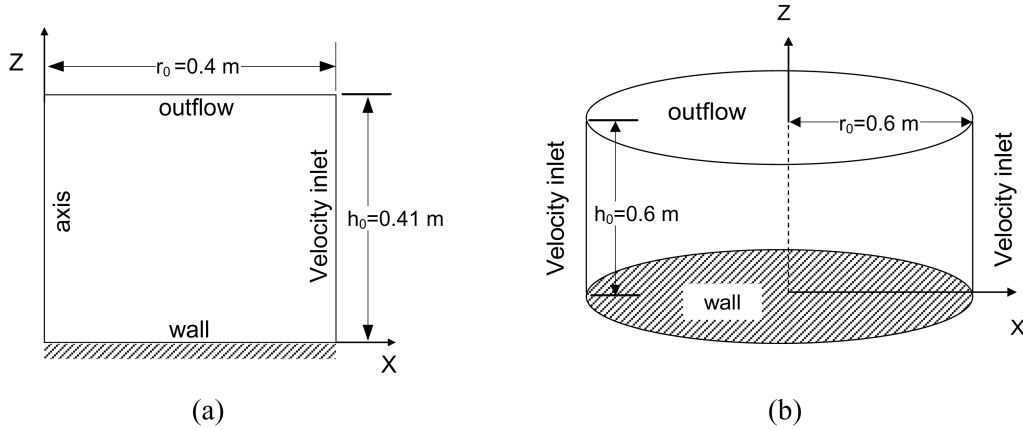


Fig. 2 Schematic of the computational domains: a) 2D simulation; b) 3D simulation

choices, however, are governed by Launder and co-workers work (Launder 1989) assuming $(1-C2-ps) / C1-ps = 0.23$ which was adopted herein. Out of all RANS models RSM is the one which is strongly recommended for highly swirling flows, Fluent 6.2. The choice of the RSM model was also motivated by our previous numerical work on downburst jets (Kim and Hangan 2007) for which multiple ring-vortices have been successfully predicted.

A segregated scheme is used to solve the governing equations, and a first order implicit formulation is selected for the temporal discretization, with a SIMPLEC (Semi Implicit Method for Pressure Linked Equation Consistent) scheme for pressure-velocity coupling and a 2nd order upwind scheme for momentum, TKE, TDR and for the Reynolds stresses. For these temporal and spatial discretization schemes, the SIMPLEC scheme typically provides better convergence compared to a PISO (Pressure-Implicit with Splitting of Operators) scheme.

At the inlet boundary, boundary layer type velocity profiles are implemented for the radial and tangential velocity components defined;

$$V_r(z) = V_0 * (z/z_0)^{1/7} \quad (1)$$

$$V_t(z) = 2 * S * V_r(z) \quad (2)$$

where V_r = radial velocity, V_t = tangential velocity, V_0 = reference velocity, z_0 = reference height and S = swirl ratio. Note that these inflow profiles are not identical to those of Baker (1981) experiments which are intrinsically related to the vortex chamber geometry rather than to atmospheric boundary layer conditions. Nevertheless an attempt was made to fit as best as possible the present boundary layer profiles to the experimental ones, by matching the radial velocity flow rates, see Fig. 3. An outflow boundary condition was used at the upper boundary. This boundary condition assumes a zero normal gradient for all flow variables except pressure (FLUENT 2005).

An “Enhanced wall treatment (FLUENT 2005) is implemented for the near wall region, which is a near-wall modeling method combining a two-layer model with enhanced wall functions. If the near-wall mesh is fine enough to be able to resolve the laminar sublayer, then the enhanced wall treatment will be identical to the traditional two-layer zonal model. A maximum wall distance $z^+ = u^* z/\nu$ of less than 1.5 for the first grid points normal to the wall was used in the wall region,

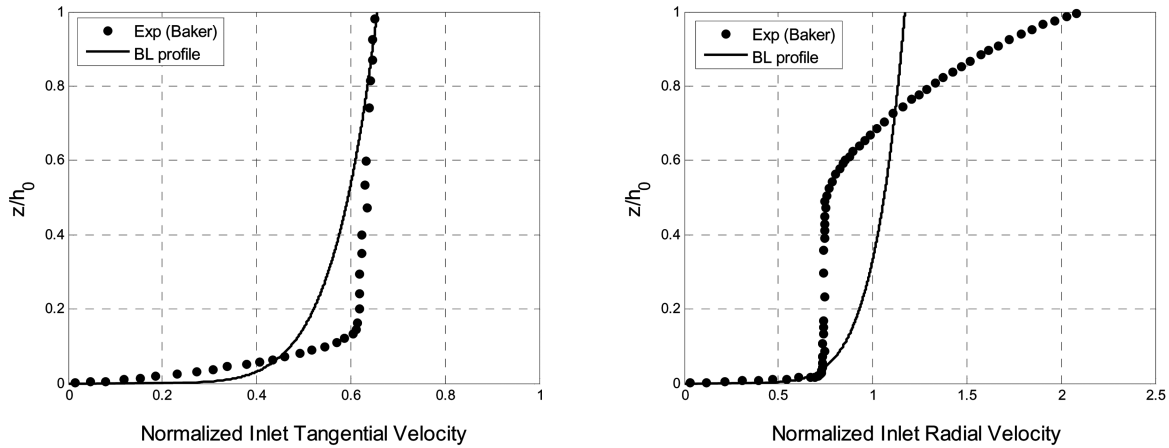


Fig. 3 Comparisons of normalized inlet tangential and radial velocity profiles used in experiment (Baker 1981) and boundary layer profiles defined in Eqs. (1) and (2)

where u^* is the friction velocity at the nearest wall, z is the distance to the wall and ν is the kinematic viscosity of air.

2.2. Benchmarking

The results of the numerical simulation were benchmarked based on experimental data (Baker 1981) obtained from a Ward-type vortex chamber for a fixed swirl ratio $S = 0.28$. Figs. 4, 5 and 6 present radial, axial and the tangential mean velocity profiles, respectively, for the experiments and for the 2D and the 3D simulations at two radial positions $r/r_0 = 0.1025$ and $r/r_0 = 0.2125$. All velocity components are normalized by the average inflow radial velocity V_r . In matching Baker's experiments we have reproduced a limited domain of the rather complex experimental apparatus. These limits were set at $r_0 = h_0 = 0.4$ meters for the 2D simulations, similar to Wilson and Rotunno (1986), and were afterwards extended to $r_0 = h_0 = 0.6$ meters for the 3D simulations.

Also, as Baker's inflow profiles are intrinsically related to the vortex chamber geometry, they were fitted with typical boundary layer profiles of same flow rate, Eqs. (1) and (2) using $V_0 = 0.34$ m/s and velocity, $z_0 = 0.025$ m. The comparison between the present set of boundary layer profiles and Baker's experimental inflow profiles is shown in Fig. 3. The velocity profiles are normalized using the reference velocity defined as $u_0 = Q / (r_0^* h_0)$ where $2\pi Q$ is the flow rate through the inlet boundary.

Overall the numerically obtained velocity field compares well with the experiments. Given the complex nature of the flow and its inherent instability, the three-dimensional simulations provide better predictions compared to the two-dimensional simulations which have the general tendency to over-predict the velocity magnitudes. Even for this relative low swirl ratio the tangential velocity component is dominant over the axial and radial components.

3. The effect of increasing swirl ratio

Once the numerical simulations were satisfactory for $S = 0.28$, they were extended to higher swirl

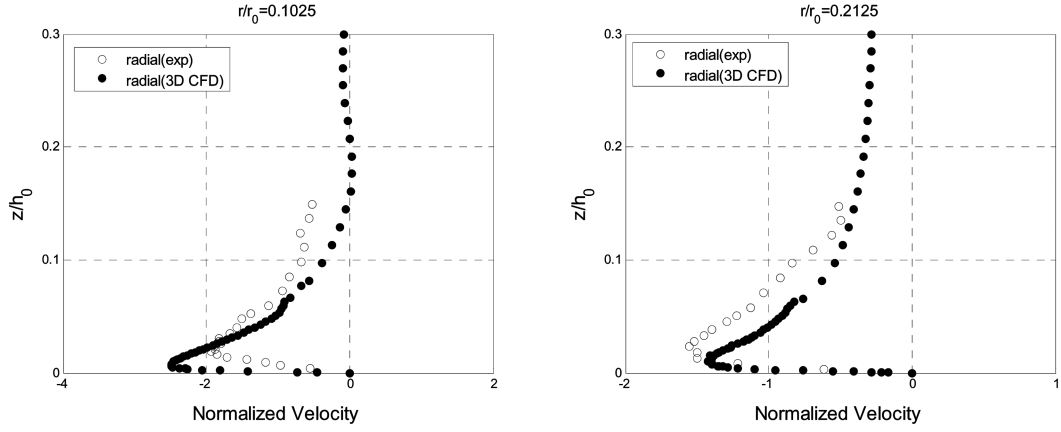


Fig. 4 Comparison of experimental and numerical (2D, 3D) radial velocity profiles, $S = 0.28$

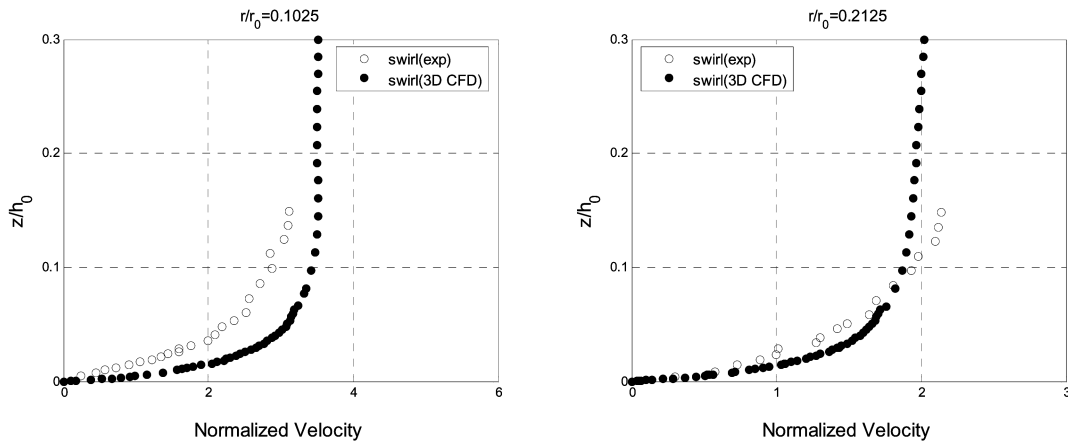


Fig. 5 Comparison of experimental and numerical (2D, 3D) axial velocity profiles, $S = 0.28$

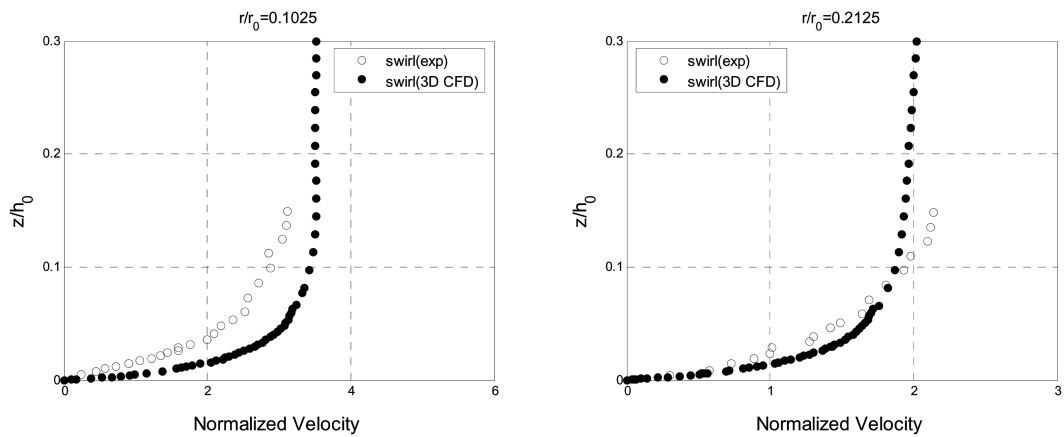


Fig. 6 Comparison of experimental and numerical (2D, 3D) tangential velocity profiles, $S = 0.28$

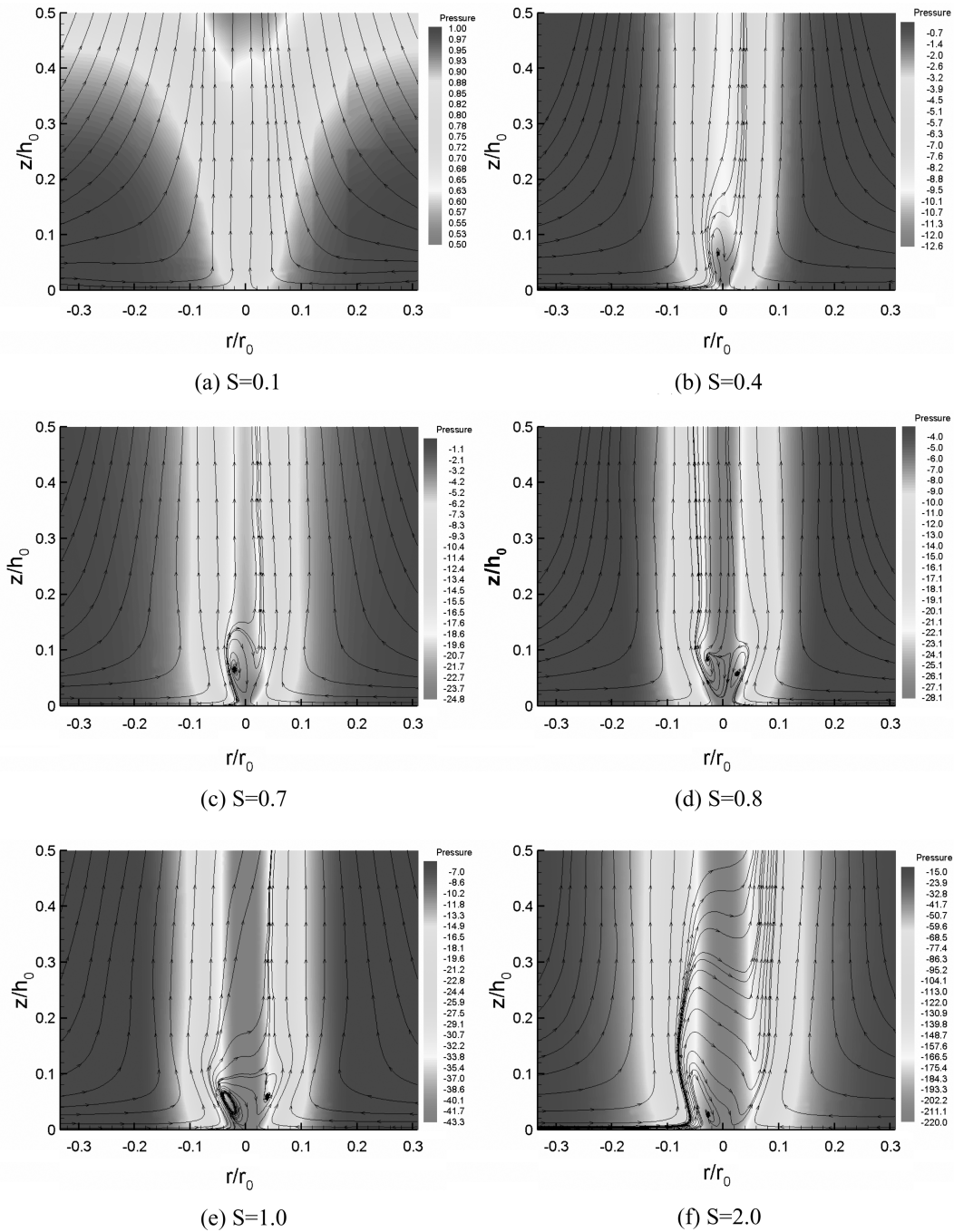


Fig. 7 Static pressure contours and streaklines for $S = 0.1, 0.4, 0.7, 0.8, 1.0$ and 2.0

ratios. Based on the comparisons for $S = 0.28$, only 3D simulations were further employed. The numerical results are presented as instantaneous superpositions of pressure contours and streaklines in Figs. 7(a) to 7(f) for swirl ratios spanning between $S = 0.1$ to $S = 2.0$.

At low swirl, $S = 0.1$, a jet-like flow is observed, Fig. 7(a), similar to the one in Fig. 1a from Lugt (1989). For $S = 0.4$ a one cell vortex break down is observed, Fig. 7(b), very close above the ground and similar to Fig. 1(b). For $S = 0.7$, the turbulent vortex has touched down and a two cell pattern starts to emerge, Fig. 7(c). At $S = 0.8$, Fig. 7(d), the two-cell structure becomes clear and similar to Fig. 1(c). As the swirl ratio increases, Fig. 7(e), $S = 1$, the vortex presents a columnar aspect and its core size increases. Finally at $S = 2$, Fig. 7(f), the streaklines show a helicoidal shape which might be related to an instability of the cylindrical shear layers and possible formation of multiple vortices. The present simulations do not provide resolved secondary vortices due to mesh resolution constraints: our equivalent full-scale mesh resolution is of the order of 4 meters or larger. Wurman (2002) shows that these secondary vortices are extremely small scale features, of the order of 10 meters, and substantially weaker than the primary tornadic flow.

4. Comparison to full scale data

An attempt was further made to match the high swirl CFD data against full scale data from the Spencer, South Dakota tornado of May 30, 1998, (Sarkar, *et al.* 2005). This full scale data was collected using the “Doppler on Wheels” system (DOW) with resolution of $30 \text{ m} \times 30 \text{ m} \times 38 \text{ m}$ (Wurman 1998).

In order to compare the CFD and the full scale observations the core radius of the columnar vortex, e.g., the radial location corresponding to the maximum tangential velocity $r_c(z)$ has been identified for each swirl ratio, see Fig. 8. Note that after vortex touch down ($S = 0.4$) a “bulge” followed by a discontinuity emerges in $r_c(z)$. For higher swirl the vortex core shows a cylindrical shape aloft and a conical shape near the surface.

The overall maximum tangential velocity $V_{t, \max} = V_t(r_{c, \max}, z_{\max})$ was matched between the full scale Doppler radar data and the CFD simulations. In this way a velocity scaling could be approximated for each swirl ratio.

Two length scales are available for matching the two data sets: the height corresponding to the maximum tangential velocity, z_{\max} , and the vortex core radius at that same height, $r_{c, \max}$. Note that the Doppler radar does not penetrate in the near-ground region and that the velocities are still increasing at the lowest level for which data is available. It was observed that $r_{c, \max}$ increases with swirl ratio while z_{\max} decreases. Therefore the scaling between full scale and the CFD simulations of the two length scale $r_{c, \max, atm} / r_{c, \max, CFD}$ and $z_{\max, atm} / z_{\max, CFD}$ converge towards the same value for $S = 2$, see Fig. 9.

Fig. 10. illustrates the matching process showing azimuthally averaged tangential wind velocity profiles from the full scale radar data and the CFD analysis by applying the velocity scaling and the z_{\max} length scaling as described above. Fig. 10. clearly shows that the overall matching between the radial profiles of tangential velocity is improving with increasing swirl. The best square fit for the outer part of the vortex ($r > r_0$) happens again close to $S = 2$. This is illustrated in Fig. 11. where $R^2 = 1 - SSE/SST$ is plotted for a function of swirl ratio where SSE is the sum of squares due to error and SST is the total sum of squares.

The matching between the Fujita scale 4 tornado and the CFD results at $S = 2$, Fig. 10(d), yields a length scale ratio of approx. 4,000 and a velocity scale of approx. 13. This gives an approximate core radius, $r_c(V_{t, \max}) \cong 0.05|_{CFD} * 4,000 \cong 200$ meters.

For the first time a relation between Fujita scale and swirl ratio may be inferred. The present analysis suggests that the full scale data attributed to a Fujita scale F4 tornado corresponds to a

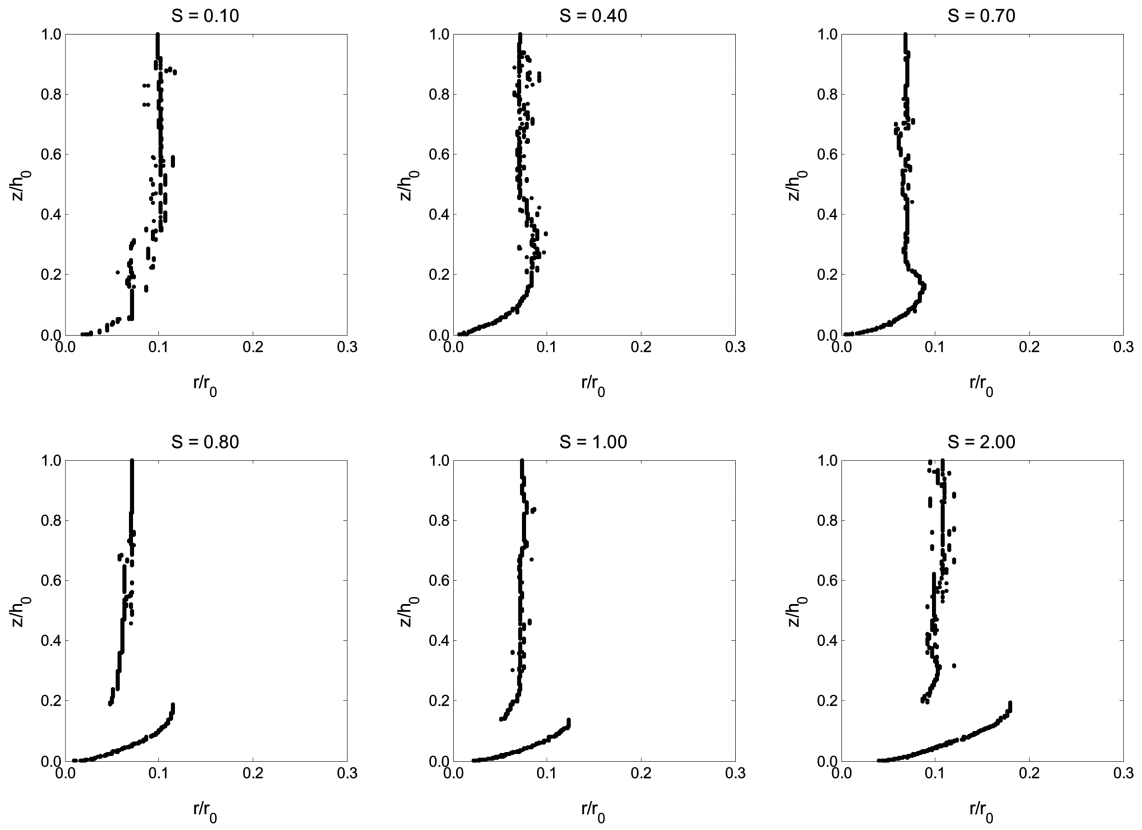


Fig. 8 Vortex core shapes for $S = 0.1, 0.4, 0.7, 0.8, 1.0$ and 2.0

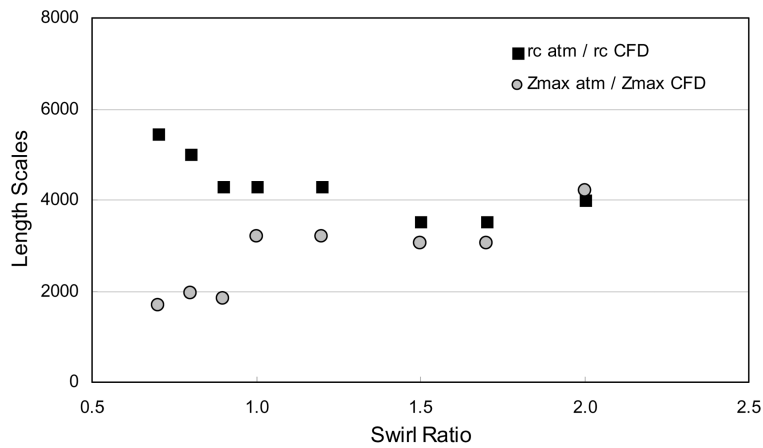


Fig. 9 Comparisons of two length scales

swirl ratio $S = 2$. Obviously further evidence is needed to validate and to extend the Fujita scale to swirl ratio relation.

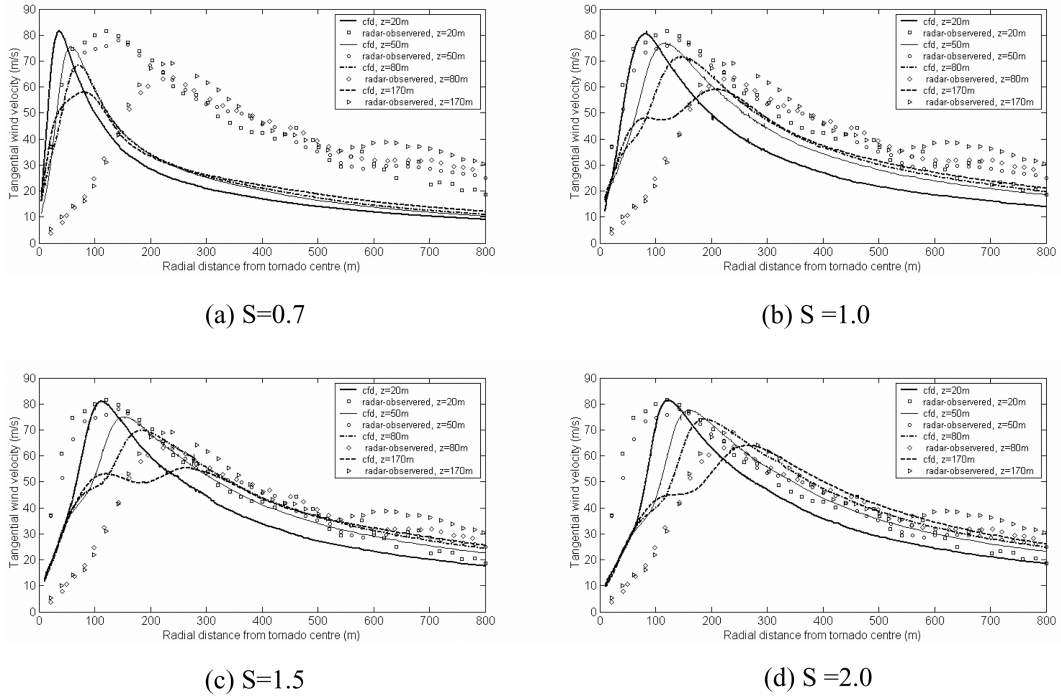


Fig. 10 Matched tangential wind velocity profiles from Doppler radar data and CFD: a) $S = 0.7$, b) $S = 1.0$, c) $S = 1.5$ and d) $S = 2.0$

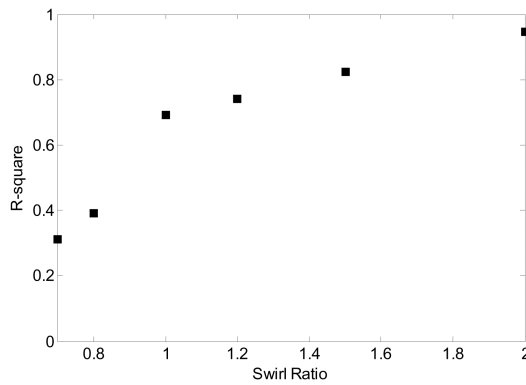


Fig. 11 R-square fit between CFD and field data for the outer part ($r > r_0$) of the tornado vortex

5. Conclusions

Engineering RANS simulations of tornado-like vortices were performed to investigate the flow dynamics as a function of swirl ratio.

Simulations for one fixed swirl ratio ($S = 0.28$) compared reasonably well with previously available TVC experimental hot-wire results. The 3D simulations clearly over-performed the axisymmetric (2D) simulations.

The benchmarked 3D model was further used to simulate tornado-like vortices for increasing swirl

ratio up to $S=2$. This range (while not complete) covers the main tornado patterns from the formation of a laminar core vortex, aloft vortex break down, to the touch down of the turbulent vortex.

Several high swirl ratio simulations were then compared to Doppler radar full scale data from a Fujita scale F4 tornado, in Spencer, South Dakota on May 30, 1998. The best fit between the CFD data and the full scale data was found for a swirl ratio of approx. $S=2$. This matching relates a fluid mechanics parameter (swirl ratio) and a forensic tornado parameter (Fujita scale) making possible the scaling of laboratory experiments to real tornados. Further Doppler Radar data is needed for the validation and extension of this relation.

Nomenclature

$C\mu$: 0.09
$C_{1\varepsilon}$: 1.44
$C_{2\varepsilon}$: 1.92
$C1-ps$: 1.8
$C2-ps$: 0.6
$C1'-ps$: 0.5
$C2'-ps$: 0.3
h_0	: height of computational domain
r_0	: radius of computational domain
r_c	: core radius
$r_{c\ max}$: core radius at z_{\max}
z_{\max}	: height corresponding to maximum tangential velocity
S	: swirl ratio, $S = 0.5 * V_t / V_r$ at inlet boundary of the computational domain (for $h_0/r_0 = 1$)
V_t	: tangential velocity
V_r	: radial velocity
V_0	: velocity at the reference height
z_0	: reference height, 0.025 m

References

- Baker, D. E. (1981), "Boundary layers in laminar vortex flows", Ph.D. thesis, Purdue University.
- Baker, G. L. and Church, C. R. (1979), "Measurements of core radii and peak velocities in modeled atmospheric vortices", *J. Atmos. Sci.*, **36**, 2413-2424.
- Bluestein, H. B., Weiss, C. C. and Pazmany, A. L. (2004), "The vertical structure of a tornado near happy, Texas, on 5 May 2002: High-Resolution, Mobile, W-band, Doppler Radar Observations", *Mon. Weather Rev.*, **132**, 2325-2337.
- Brooks, H. E. (2004), "On the relationship of tornado path length and width to intensity", *Weather Forecast.*, **19**, 310-319.
- Church, C. R., Snow, J. T., Baker, G. L. and Agee, E. M. (1979), "Characteristics of tornado-like vortices as a function of swirl ratio: A laboratory investigation", *J. Atmos. Sci.*, **36**, 1755-1776.
- Church, C. J., Snow, J. T. and Agee, E. M. (1977), "Tornado vortex simulation at Purdue University", *Bull. Amer. Meteor. Soc.*, **58**, 900-908.
- Davies-Jones, R. P. (1973), "The dependence of core radius on swirl ratio in a tornado simulator", *J. Atmos. Sci.*, **30**, 1427-1430.
- Fiedler, B. H. and Rotunno, R. (1986), "A theory for the maximum windspeeds in tornado-like vortices", *J. Atmos. Sci.*, **43**, 2328-2340.
- Fluent 6.2 User's Guide (2005), Fluent Inc., Lebanon.
- Fujita, T. T. (1981), "Tornadoes and downbursts in the context of generalized planetary scales", *J. Atmos. Sci.*, **38**, 1511-1534.

- Kim, J-D., Hangan, H. (2007), "Numerical simulations of impinging jets with application to downbursts", *J. Wind Eng. Ind. Aerodyn.*, **95**(4), 279-298.
- Lauder, B. E. (1989), "Second-moment closure and its use in modeling turbulent industrial flows", *Int. J. Numer. Methods Fluids*, **9**, 963-965.
- Lee, W-C., Wurman, J. (2005), "Diagnosed three-dimensional axisymmetric structure of the Mulhall tornado on 3 May 1999", *J. Atmos. Sci.*, **62**, 2373-2394.
- Lewellen, W. S. (1963), "A solution for three-dimensional vortex flows with strong circulation", *J. Fluid Mech.*, **14**, 420-432.
- Lewellen, W. S., Lewellen, D. C. and Sykes, R. I. (1997), "Large-eddy simulation of a tornado's interaction with the surface", *J. Atmos. Sci.*, **54**, 581-605.
- Lewellen, D. C., Lewellen, W. S. and Xia, J. (2000), "The influence of a local swirl ratio on tornado intensification near the surface", *J. Atmos. Sci.*, **57**, 527-544.
- Lewellen, D. C. and Lewellen, W. S. (2007), "Near-surface intensification of tornado vortices", *J. Atmos. Sci.*, **64**, 2176-2194.
- Lim, T. T. and Cui, Y. D. (2003), "On the generation of a spiral-type vortex breakdown in an enclosed cylindrical container", *Phys Fluids*, **17**, 044-105.
- Lugt, H. (1989), "Vortex breakdown in atmospheric columnar vortices", *Bull. Amer. Meteor. Soc.*, **70**, 1526-1537.
- Lund D. E. and Snow, J. (1993), "The tornado: its structure, dynamics, prediction and hazards", *Geophys. Monogr. Ser.* **79**, 297-306.
- Nolan, D. S. and Farrell, B. F. (1999), "The structure and dynamics of tornado-like vortices", *J. Atmos. Sci.*, **56**, 2908-2936.
- Nolan, D. S. (2005), "A new scaling for tornado-like vortices", *J. Atmos. Sci.*, **62**, 2639-2646.
- Rotunno, R. (1979), "A Study in tornado-like vortex dynamics", *J. Atmos. Sci.*, **36**, 140-155.
- Sarkar, P., Haan, F., Gallus, Jr., W., Le, K. and Wurman, J. (2005), "Velocity measurements in a laboratory tornado simulator and their comparison with numerical and full-scale data", *37th Joint Meeting Panel on Wind and Seismic Effects*, Tsukuba, Japan, May 2005.
- Selvam, R. P. and Millet P. C. (2003), "Computer modeling of tornado forces on buildings", *Wind Struct.*, **6**, 209-220.
- Selvam, R. P. and Millet, P. C. (2005), "Large eddy simulation of the tornado-structure interaction to determine structural loads", *Wind Struct.*, **8**, 49-60.
- Serre, E. and Bantoux P. (2002), "Vortex breakdown in a three-dimensional swirling flow", *J. Fluid Mech.*, **459**, 347-370.
- Snow J. T. (1982), "A review of recent advances in tornado vortex dynamics", *Rev. Geophys. Space Phys.*, **20**, 953-964.
- Smith, D. R. (1987), "Effect of boundary conditions on numerically simulated tornado-like vortices", *J. Atmos. Sci.*, **44**, 648-656.
- Twisdale L. A. and Vickery P. J. (1992), "Research on thunderstorm wind design parameters", *J. Wind Eng. Ind. Aerodyn.*, **41-44**, 545-556.
- Wan, C. and Chang, C. (1972), "Measurement of the velocity field in a simulated tornado-like vortex using a three-dimensional velocity probe", *J. Atmos. Sci.*, **29**, 116-127.
- Wang, H., James, D., Letchford, C. W., Peterson, R. and Snow, J. (2001), "Development of a prototype tornado simulator for the assessment of fluid-structure interaction", *First American Conference on Wind Engineering*, 4-6 June, 2001, Clemson, SC.
- Ward, N. B. (1972), "The exploration of certain features of tornado dynamics using a laboratory model", *J. Atmos. Sci.*, **29**, 1194-1204.
- Wilson, T. and Rotunno, R. (1986), "Numerical simulation of a laminar end-wall vortex and boundary layer", *Phys. Fluids*, **29**, 3993-4005.
- Wurman, J. (1998), "Preliminary results from the ROTATE-98 tornado study", *Preprints, 19th Conf. on Severe Local Storms*, Minneapolis, MN, 14-18 September, 120-123.
- Wurman, J. and Gill, S. (2000), "Finescale radar observations of the Dimmitt, Texas (2 June 1995), Tornado", *Mon. Weather Rev.*, **128**, 2135-2164.
- Wurman, J. (2002), "The multiple-vortex structure of a tornado", *Weather Forecast.*, **17**, 473-500.
- Xia, J., Lewellen, W. S. and Lewellen, D. C. (2003), "Influence of Mach number on tornado corner flow dynamics", *J. Atmos. Sci.*, **60**, 2820-2825.